Available online at www.sciencedirect.com
SCIENCE DIRECT
Journal of Molecular Catalysis A: Chemical 238 (2005) 158–162
JOURNAL OF MOLECULAR CATALYSIS A: CHEMICAL
www.elsevier.com/locate/molcata

Direct synthesis of dimethyl carbonate on H_3PO_4 modified V_2O_5

X.L. Wu [a], M. Xiao [a], Y.Z. Meng [a,*], Y.X. Lu [b,1]

[a] *State Key Laboratory of Optoelectronic Materials and Technologies, Sun Yat-Sen University, Guangzhou 510275, PR China*
[b] *Department of Chemistry, National University of Singapore, 3 Science Drive 3, Singapore 117543, Singapore*

Received 5 April 2005; accepted 17 May 2005
Available online 27 June 2005

Abstract

The catalytic properties of modified V_2O_5 catalysts for the dimethyl carbonate (DMC) synthesis from CO_2 and CH_3OH were investigated. Experimental results showed that the modified V_2O_5 catalysts were effective for the direct and selective synthesis of DMC from carbon dioxide and methanol. The characterization of modified V_2O_5 catalysts was performed by means of X-ray diffraction (XRD), thermogravimetric (TG) and diffuse reflectance FTIR (DRIFT) spectra. XRD patterns showed that the crystal phase changed from orthorhombic to orthorhombic-tetragonal double phase. TG results showed that the weaker acid sites increased when V_2O_5 was treated with varying H_3PO_4 contents. DRIFT spectra of the CO_2 and CH_3OH absorbed on catalysts indicated that both CO_2 and CH_3OH were effectively activated on the catalysts. Finally, the experiment results demonstrated that the crystal phase of the catalyst influenced greatly on the reaction yield and selectivity of DMC.

Keywords: Dimethyl carbonate (DMC); DRIFT; V_2O_5

1. Introduction

Dimethyl carbonate (DMC) is an environmentally benign compound and unique intermediate with versatile chemical reactivity. The synthesis of DMC has attracted much attention in terms of a non-toxic substitute for dimethyl sulfate and phosgene, which are toxic and corrosive methylation and carbonylating agents [1–3]. In addition, DMC can be used as solvent, alkylation agents, fuel additive and in the synthesis of aromatic polycarbonate resins [4,5]. The traditional synthesis of DMC used to require phosgene as a reagent. However, phosgene has serious disadvantages such as intense toxicity. It is expensive to prepare phosgene from high energy reagents, like chlorine and carbon monoxide, together with serious corrosion of used equipment. Another route for the synthesis of DMC is the oxidative carbonylation of CH_3OH with CO and oxygen in the presence of copper and/or palladium as catalyst [6,7]. In recent years, direct synthesis of DMC from CO_2 and CH_3OH is the most attractive way due to the low-cost of CO_2 and methanol [8]. In this sense, the conversion of CO_2 to industrially useful compounds has been a challenge for synthetic chemist and has recently attracted much interest in the view of the so-called “Sustainable Society” and “Green chemistry” [9].

Many catalysts have been used for the synthesis of DMC from CO_2 and methanol including organometallic compounds and inorganometallic compounds, such as $BuSn(OMe)_2$ [10,11], metal(IV)tetra-alkoxide [12], magnesium dialkoxide [13], potassium carbonate [14], zirconia [15], CeO_2–ZrO_2 [16] and $Ni(CH_3COO)_2$ [9]. However, the yield of DMC was reported to be low because of the limitation of the reaction thermo-dynamic, even in the presence of dehydrates and additives such as $CaCl_2$ [17], 2.2-dimethoxy propane (DMP) [16] acetals [9,18] and molecular sieves [19]. More recently, the direct synthesis of DMC from CO_2 and CH_3OH has been performed under supercritical

* Corresponding author. Tel.: +86 20 84114113; fax: +86 20 84114113.
E-mail addresses: stdpmeng@zsu.edu.cn (Y.Z. Meng), chmlyx@nus.edu.sg (Y.X. Lu).
[1] Tel.: +65 68741569; fax: +65 67791691.

1381-1169/$ – see front matter © 2005 Elsevier B.V. All rights reserved.
doi:10.1016/j.molcata.2005.05.018

condition [20,21]. The rigorous method is difficult to control. Therefore, the gaseous reaction between CO_2 and CH_3OH has been investigated because gaseous reaction can partly circumvent the self-limitation of this reaction [22]. In this paper, the direct synthesis of DMC from gaseous methanol and CO_2 was studied using modified V_2O_5 as catalyst. The synthesis and characteristic of the modified V_2O_5 catalyst were.

2. Experimental

2.1. Materials

CH_3OH (A.R. Xiehe Co., Tianjin, China), CO_2 (99.9% SGIG Co., Shanghai, China), V_2O_5 (A.R. Lijiadian Agent Co., Beijing, China), aqueous H_3PO_4 solution (85% A.R. Guanghua Agent Co., Shantou, China), NH_3 (A.R. Xinguang Agent Co., Beijing, China).

2.2. DMC synthesis from CO_2 and CH_3OH

A continuous tubular fixed-bed micro-gaseous reactor (15 mm I.D.) operated at 0.6 MPa total pressure was used for the assessment of synthesized catalysts. The typical procedure is as follows: 0.5 g of catalyst was flatwise placed on the glass fiber stuffed in the reactor, CO_2 and CH_3OH were then purged into the reactor. CH_3OH was introduced into the reactor using CO_2 flow. The ratio of CH_3OH to CO_2 can be easily controlled via the vaporization temperature of CH_3OH and the flux of CO_2. A molar ratio of 2:1 of CH_3OH:CO_2 was selected for all reaction entries. The mass of CH_3OH and CO_2 was controlled with gas-flow meter. The reaction was performed at varying temperatures. Resulting products were absorbed in deionized water and analyzed by gas chromatograph (Techcomp GC7890) equipped with a capillary column (length: 15 m, I.D.: 0.25 mm) and a flame ionization detector (FID).

2.3. Catalyst preparation

V_2O_5 was prepared by calcining a commercially available V_2O_5 at 732 K for 3 h in air. Phosphoric acid modified V_2O_5 catalyst were prepared by impregnating calcined V_2O_5 with an 85% aqueous H_3PO_4 solution. The resulting product was dried at 393 K for 3 h, followed by calcination at 673 K for another 3 h in air. These catalysts are represented as H_3PO_4/V_2O_5. The content of H_3PO_4 is denoted as the molar ratio P/V in parentheses (e.g., P/V = 0.20).

2.4. Catalyst characterization

2.4.1. X-ray diffractive (XRD)

X-ray analysis was carried out on a D/Max-IIIA power diffractometer in a step mode between 10° and 60° 2θ using Cu Kα_1 radiation. The mean crystallite degree was calculated from the half-width of the reflection.

2.4.2. Thermal analysis

Thermogravimetric (TG) studies of samples were performed on a Perkin Elmer Pyris Diamond SII thermoanalyer in N_2 at a heating rate of 5 K min^{-1} and using α-Al_2O_3 as a reference. TG profiles of NH_3 desorption and CO_2/CH_3OH desorption on H_3PO_4/V_2O_5 were carried out in N_2 flow at 673 K for 0.5 h; NH_3 or CO_2/CH_3OH was introduced under atmospheric pressure at 673 K with N_2 as a carrier gas and kept 0.5 h at this temperature. Before the measurement, the samples were evacuated for 0.5 h at room temperature.

Diffuse reflectance FTIR (DRIFT) spectra. DRIFT spectra measurements were carried out on a Bruker EQUINOX 55 FTIR instrument equipped with a diffuse reflectance unit. DRIFT analysis was performed in a pure N_2 flow at 0.2 MPa at a heating rate of 5 K min^{-1} from 298 to 473 K, followed by holding at 473 K for 30 min. Finally, CH_3OH and/or CO_2 were introduced instead of N_2 at this temperature for 30 min at 0.2 MPa. The same process was employed for NH_3 that was carried by N_2 flow.

3. Results and discussion

3.1. Catalytic activity for the direct synthesis of DMC from CO_2 and CH_3OH

Table 1 lists the conversion of CH_3OH and the dependence of DMC yield and selectivity on H_3PO_4 content. The yield and selectivity of DMC, as well as the conversion of CH_3OH, increased with increasing H_3PO_4 content at low P/V ratios. The DMC yield and selectivity reached a maximum value at P/V = 0.20 and then decreased with further increasing H_3PO_4 content.

Fig. 1 shows the conversion of methanol and the selectivity of DMC with respect to reaction temperature on V_2O_5 and H_3PO_4/V_2O_5 (P/V = 0.05, 0.2 and 0.5) catalysts. Fig. 1a shows that the conversion of methanol on V_2O_5 was very low, however, H_3PO_4 modified V_2O_5 enhanced greatly the activity at all reaction temperatures. The conversion of methanol

Table 1
The dependence of DMC yield and selectivity and the conversion of CH_3OH on H_3PO_4 contents

Molar ratio (P/V)	The amount of DMC (mmol)	Conversion of CH_3OH (%)	Selectivity of DMC (%)
0	0.45	0.200	89.63
0.010	0.45	0.203	88.60
0.025	0.60	0.265	90.61
0.050	2.10	0.912	92.05
0.150	3.40	1.478	92.01
0.200	4.50	1.954	92.12
0.300	3.10	1.374	90.23
0.500	2.90	1.277	90.82

Reaction conditions: CH_3OH/CO_2 = 500/250 mmol, catalyst weight: 0.5 g, reaction temperature: 413 K. CH_3OH was introduced in gaseous phase, carried by CO_2 flow, the ratio of CH_3OH to CO_2 was controlled by adjusting the temperature of CH_3OH.

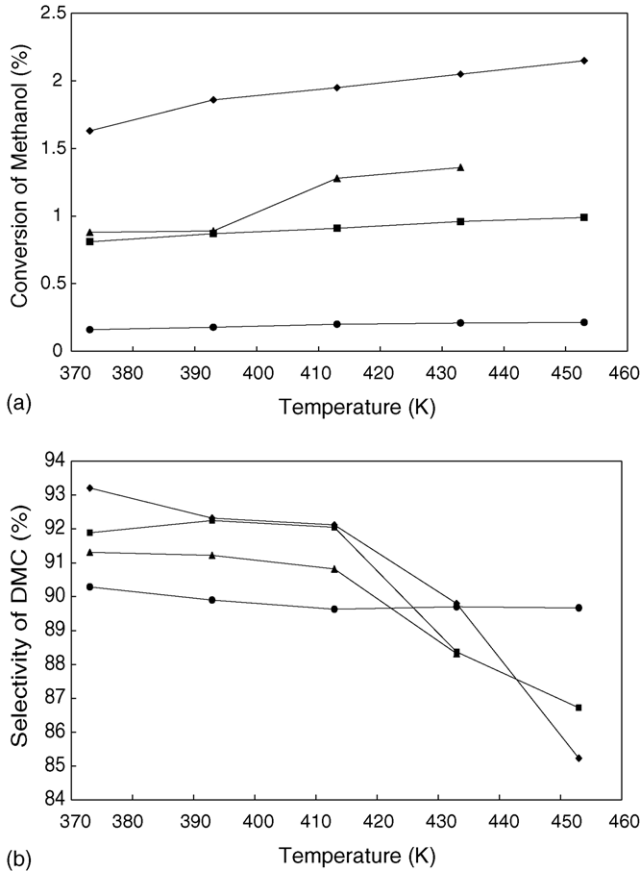

Fig. 1. (a) The conversion of methanol and (b) the selectivity of DMC on the content of H_3PO_4 (P/V = 0, ●; 0.05, ■; 0.20, ♦; 0.5, ▲) and reaction temperature.

on H_3PO_4/V_2O_5 (P/V = 0.20) at 453 K was about 8–9 times more than that on neat V_2O_5. Fig. 1b shows that the selectivity of DMC decreased with increasing of temperature on all catalysts. The selectivity of DMC was improved when the catalysts was modified with H_3PO_4. When P/V = 0.2 the result are better than that of any others. It seems that the DMC yield on H_3PO_4 modified V_2O_5 at 413 K reached an equilibrium value.

3.2. Structure of H_3PO_4 modified V_2O_5

XRD patterns of H_3PO_4/V_2O_5 catalysts with various H_3PO_4 contents are shown in Figs. 2 and 3. The peaks at $2\theta = 15.5$, 20.4, 21.7, 26.3, 31.1° correspond the characteristic orthorhombic phase of V_2O_5, while peaks at $2\theta = 12.5$, 28.9, 31.1° are the characteristic tetragonal phase of V_2O_5. For H_3PO_4/V_2O_5 catalysts (P/V = 0.01, 0.025, 0.05), only orthorhombic phase were observed. When increasing P/V ratio to 0.15, the orthorhombic phase gradually decreased with further increasing H_3PO_4 content, while the tetragonal phase increased with increasing H_3PO_4 content. Both orthorhombic and tetragonal phases were predominantly formed for H_3PO_4/V_2O_5 catalysts when P/V ratio >0.15. In case of P/V ratio being 0.5, there was a new strong peak

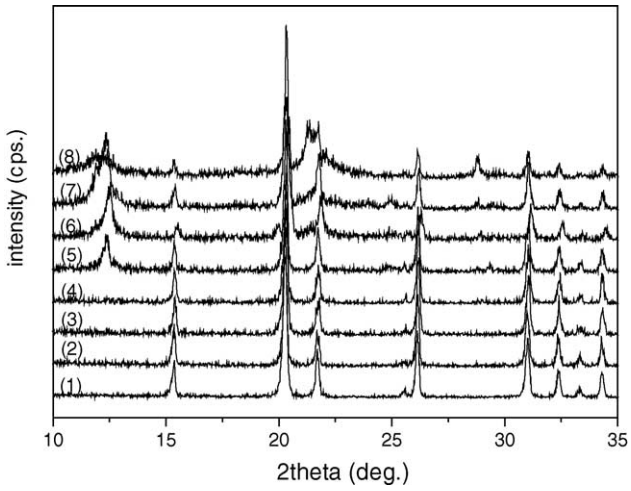

Fig. 2. XRD patterns of H_3PO_4/V_2O_5 catalysts with varying H_3PO_5 contents in the range of $2\theta = 10$–35°: (1) P/V = 0, (2) P/V = 0.01, (3) P/V = 0.025, (4) P/V = 0.05, (5) P/V = 0.15, (6) P/V = 0.2, (7) P/V = 0.3, (8) P/V = 0.5.

located at $2\theta = 21.3°$. The related structure for this new peak remains unclear. The characteristic peak of tetragonal phase at $2\theta = 18.1°$, as shown in trace 8 of Fig. 2, became weak, implying that its crystallinity decreased.

3.3. Adsorption behavior of H_3PO_4 modified V_2O_5

Fig. 4 shows the TG profiles of V_2O_5 and H_3PO_4/V_2O_5 (P/V = 0.20) with adsorbed NH_3. Desorption of NH_3 on V_2O_5 occurred only at near room temperature, while desorption of NH_3 on H_3PO_4/V_2O_5 (P/V = 0.2) happened in a broader temperature range from room temperature to 600 K. The desorption rate in range of 293–355 K was higher than that in range of 355–600 K. These indicated that there were several different bondings between NH_3 and H_3PO_4/V_2O_5, which were stronger than that between NH_3 and neat V_2O_5. It is

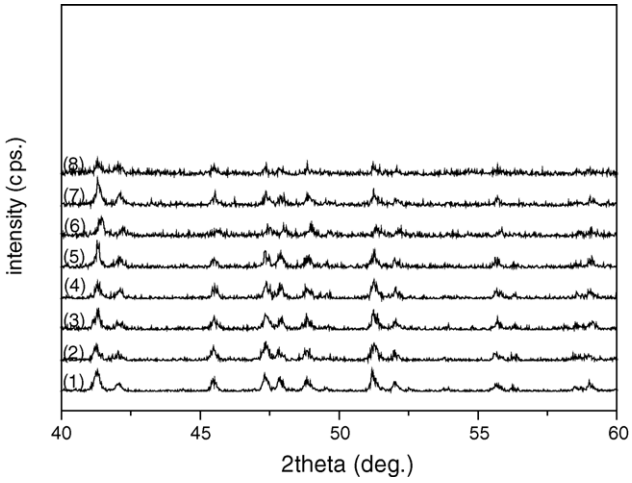

Fig. 3. XRD patterns of fresh H_3PO_4/V_2O_5 catalysts with varying H_3PO_5 contents in the range of $2\theta = 40$–60°: (1) P/V = 0, (2) P/V = 0.01, (3) P/V = 0.025, (4) P/V = 0.05, (5) P/V = 0.15, (6) P/V = 0.2, (7) P/V = 0.3, (8) P/V = 0.5.

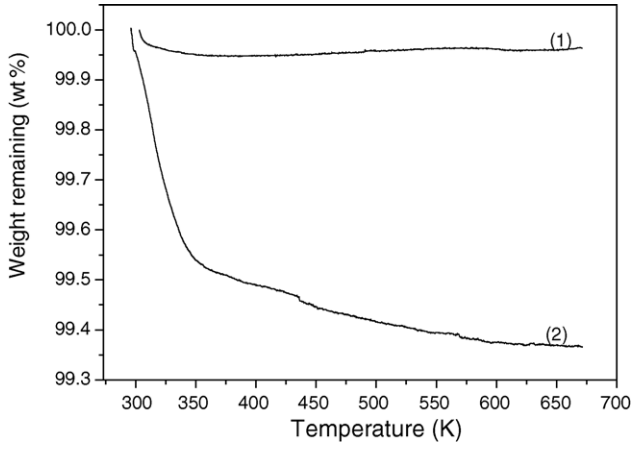

Fig. 4. TG curves of (1) on V_2O_5 with absorbed NH_3 and (2) H_3PO_4/V_2O_5 (P/V = 0.20) with absorbed NH_3. TG was run at heating rate of 5 K min^{-1} and in N_2.

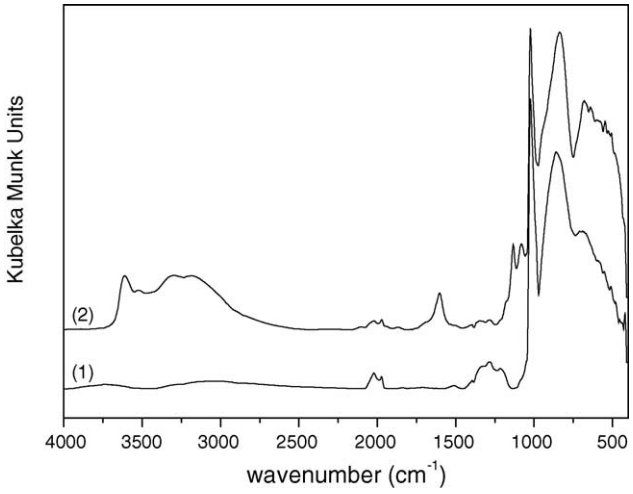

Fig. 6. DRIFT spectra of (1) V_2O_5 and (2) H_3PO_4/V_2O_5.

believed that the reinforcement of acid sites on the surface of H_3PO_4 modified V_2O_5 accounts for the stronger bondings. More desorpted NH_3 on H_3PO_4/V_2O_5 (P/V = 0.2) was observed in lower temperature range when compared with neat V_2O_5. This demonstrated that H_3PO_4 modified V_2O_5 resulted in an increase in the number of weak acid sites. These acid sites on H_3PO_4/V_2O_5 can be attributed to the weak Brønsted acid sites near P atoms.

Fig. 5 shows the TG profiles of H_3PO_4/V_2O_5 (P/V = 0.20) with absorbed CO_2 and CH_3OH. Desorption of CO_2 and CH_3OH on H_3PO_4/V_2O_5 was observed in a wide temperature range from room temperature to 400 K. These meant that there were also different kinds of bondings between CH_3OH/CO_2 and H_3PO_4/V_2O_5. The behavior was similar with that between NH_3 and H_3PO_4/V_2O_5. The active sites are believed to serve as the catalytic sites for the direct synthesis of DMC from CO_2 and CH_3OH.

DRIFT spectra of V_2O_5 and H_3PO_4/V_2O_5 (P/V = 0.20) are shown in Fig. 6. The structure of V_2O_5 changed when subjected to H_3PO_4 treatment. Four new bands at 3611, 3525, 3295 and 3165 cm^{-1} in the range of 3000–3750 cm^{-1} can be observed in the DRIFT spectra of H_3PO_4/V_2O_5 when compared with neat V_2O_5. These new bands are related with the stretching modes of dissociated hydroxyl groups. In the region of 2200–900 cm^{-1}, the intensities of 2022, 1973, 1395 and 1287 cm^{-1} bands decreased with increasing H_3PO_4 content. Bands at 1214 and 1500 cm^{-1} disappeared in the spectrum of H_3PO_4/V_2O_5 in trace 2 of Fig. 6. New bands at 1604, 1349, 1134 and 1081 cm^{-1} were detectable as shown in trace 2 of Fig. 6. These bands correspond to the stretching modes of P–O–V bonds. The band at 861 cm^{-1} (trace 1 in Fig. 6), which is associated with vibration of bond V–O–V, shifted to 839 cm^{-1}. Band at 694 cm^{-1} of trace 1 in Fig. 6 shifted to 680 cm^{-1} of trace 2 in Fig. 6.

The DRIFT spectra of V_2O_5 (trace 1) and V_2O_5–NH_3 (trace 2) and the DRIFT spectra of H_3PO_4/V_2O_5 (trace 1) and H_3PO_4/V_2O_5 (P/V = 0.20)–NH_3 (trace 2) are shown in Fig. 7A and B, respectively. In Fig. 7A, the band at 3008 cm^{-1} can be seen in trace 2, which was assigned to

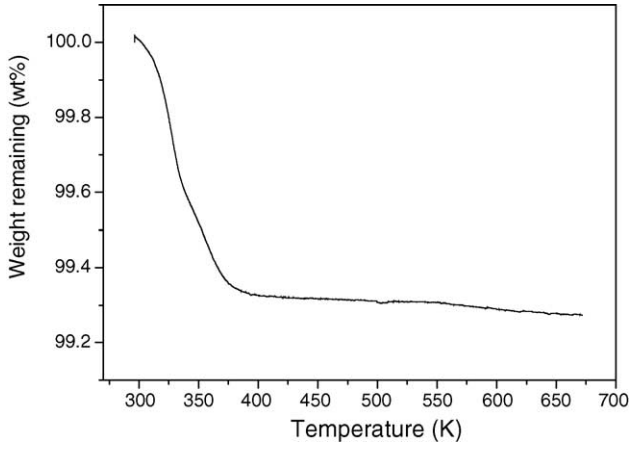

Fig. 5. TG profiles of H_3PO_4/V_2O_5 with adsorbed CO_2 and CH_3OH. TG was run at heating rate of 5 K min^{-1} and in N_2.

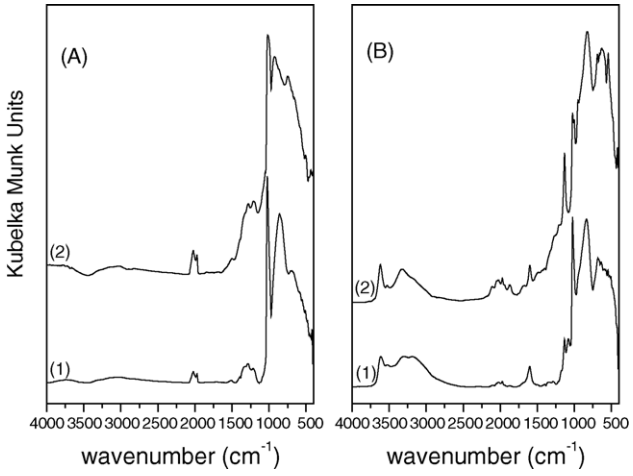

Fig. 7. DRIFT spectra of (1) V_2O_5 and (2) V_2O_5–NH_3 in (A) as well as (1) H_3PO_4/V_2O_5 and (2) H_3PO_4/V_2O_5–NH_3 in (B).

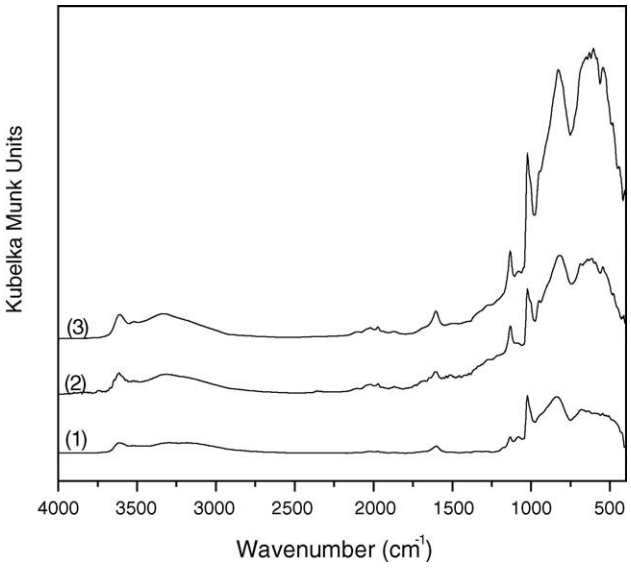

Fig. 8. DRIFT spectra of (1) H_3PO_4/V_2O_5, (2) H_3PO_4/V_2O_5─CH_3OH/CO_2 and (3) H_3PO_4/V_2O_5─CH_3OH.

N–H vibration of $–NH_3^+$. From Fig. 7B bands at 3611 and 3295 cm^{-1} shifted to 3618 and 3322 cm^{-1} when NH_3 was absorbed on H_3PO_4/V_2O_5 (P/V = 0.2). The band at 3165 cm^{-1} disappeared, but two new bands at 2108 and 1873 cm^{-1} appeared in trace 2 of Fig. 7B, which correspond to the vibration of unbonded electron of N matched to vacant orbit of $V^{\delta+}$. The intensity of band at 1025 cm^{-1} decreased greatly, while a new band at 1020 cm^{-1} was observed when NH_3 was absorbed. These bands were thought to be V=O bond. The band at 839 cm^{-1} (trace 1 in Fig. 7B) shifted to 826 cm^{-1} (trace 2 in Fig. 7B) with an increased intensity.

Fig. 8 shows the DRIFT spectra of H_3PO_4/V_2O_5, H_3PO_4/V_2O_5–CH_3OH and H_3PO_4/V_2O_5–CH_3OH/CO_2 compounds. In the range of 3750–3000 cm^{-1}, dissociated hydroxyl group vibration shifted from 3611 to 3614 cm^{-1} after CH_3OH was absorbed on the catalyst. The band at 3295 shifted to 3335 and 3312 cm^{-1} when absorbing first CH_3OH and then CO_2 on the catalyst. No peak in the region of 3000–2500 cm^{-1} was detectable for all spectra. New bands at 1875 and 1517 cm^{-1} in the spectra of H_3PO_4/V_2O_5 (P/V = 0.2)–CH_3OH/CO_2 were assigned to the methoxyl carbonate species. The bands at 1396, 1349 and 1288 cm^{-1} are related with the vibration of P=O that disappeared when CH_3OH and CO_2 was absorbed on the catalyst. This indicated that P served for the activation of CO_2 and CH_3OH. The intensity decrease of V=O bond at 1024 cm^{-1} also demonstrated that V=O participated the activation of CO_2 and CH_3OH. The band at 958 cm^{-1} in the spectra of H_3PO_4/V_2O_5–CH_3OH (trace 3 in Fig. 8) became stronger when CO_2 was absorbed onto the catalyst. The band at 839 cm^{-1} shifted to 828 cm^{-1} with the introduction of CH_3OH followed by shifting to 819 cm^{-1} with subsequent introduction of CO_2 on the catalyst. This band belongs to the vibration of V–O–P band, showing that V–O–P can activate CO_2 and CH_3OH.

4. Conclusion

(1) When P/V > 0.15, the crystal phase of H_3PO_4/V_2O_5 changed from single orthorhombic phase to a combined orthorhombic/tetragonal phase. The bicrystal phase in H_3PO_4 modified V_2O_5 is effective for the DMC synthesis from CO_2 and CH_3OH.
(2) The optimum composition of H_3PO_4/V_2O_5 with P/V = 0.15–0.50 showed effective activation of both CO_2 and CH_3OH.
(3) The direct interaction between V and P is essential for the formation of weak Brønsted acid sites. Brønsted acid sites on H_3PO_4/V_2O_5 are more effective than Lewis acid sites on V_2O_5 for the CH_3OH activation on the acid sites. The reaction of the activated CH_3OH with methyl carbonate species then gives DMC.

Acknowledgements

We thank the Ministry of Science and Technology of China (Grant No. 2002BA653C), Natural Science Foundation of Guangdong Province (Excellent Team Project, Grant No. 015007), Key Strategic Project of Chinese Academy of Sciences (Grant No. KJCX2-206B) and Key Project of Guangzhou Science and Technology Bureau (Grant No. 2001-z-114-01) for financial support of this work.

References

[1] Y. Ono, Appl. Catal. A: Gen. 155 (1997) 133.
[2] M. Aresta, E. Quaranta, Chemtech (1997) 32.
[3] A.A. Shaikh, S. Sivaram, Chem. Rev. 76 (1996) 951.
[4] P. Jessop, G. Ikariya, et al., Chem. Rev. 99 (1999) 475–494.
[5] S. Neil Isaaca, Brian O'Sullivan, et al., Tetrahedron 55 (1999) 11949–11956.
[6] U. Rorrano, R. Tesei, et al., Ind. Eng. Chem. Prod. Res. Dev. 19 (1980) 396.
[7] M.Y. Lee, D.C. Park, Stud. Sci. Catal. 66 (1991) 631.
[8] T.S. Zhao, Y.Z. Han, et al., Fuel Process. Technol. 62 (2000) 187–194.
[9] J.C. Choi, T. Sakakura, et al., J. Am. Chem. Soc. 121 (1999) 3793–3794.
[10] J. Kizlink, Collect. Czech. Chem. Commum. 58 (1993) 1399.
[11] K. Ko, O. Fujumaro, Jpn. Kakai Tokkyo Koho (1995) JP95224011.
[12] J. Kizlink, I. Pastucha, Collect. Czech. Chem. Commun. 60 (1995) 687.
[13] X. Gui, et al., J. Chem. Eng. Chin. Univ. 12 (1998) 152.
[14] S. Fang, K. Fujimoto, Appl. Catal. A 142 (1996) L1.
[15] K. Taek Jung, T. Alexic Bell, Top. Catal. 20 (2002) 97–105.
[16] K. Tomishige, K. Kunimori, Appl. Catal. A: Gen. 237 (2002) 103–109.
[17] Q. Jiang, T. Li, et al., Chin. J. Appl. Chem. 16 (5) (1999) 115–116.
[18] J.C. Choi, L.N. He, et al., Green Chem. 4 (2002) 230–243.
[19] Z.S. Hou, et al., Green Chem. 4 (2002) 467–471.
[20] R. Noyori, Chem. Rev. 99 (2) (1999) 1.
[21] P.G. Jessop, W. Leitner (Eds.), Chemical Synthesis using Supercritical Fluids, Wiley–VCH, Weinheim, 1999.
[22] C. Feng, S.H. Zhong, Catal. Today 82 (2003) 83–90.